PAPER • **OPEN ACCESS**

An Experimental and Numerical Evaluation of Natural Frequencies and Mode Shapes using Vibration Isolator to Transport “Satellite Model–Plate Connecting Interface” System

To cite this article: Abbas Waheed Dahham *et al* 2021 *IOP Conf. Ser.: Mater. Sci. Eng.* **1094** 012020

View the article online for updates and enhancements.

You may also like

- Development of Vibration Isolator Magnetorheological Elastomer Based
G Priyandoko, P Suwandono, NR Ismail et al.
- Design and Development of Structural Parameter Identification Software for Nonlinear Vibration Isolators
Chen Meng, Shiheng Xu and Xiaoxu Zhang
- A real-time controllable electromagnetic vibration isolator based on magnetorheological elastomer with quasi-zero stiffness characteristic
Shaogang Liu, Lifeng Feng, Dan Zhao et al.



This content was downloaded from IP address 95.14.120.62 on 13/09/2023 at 12:41

An Experimental and Numerical Evaluation of Natural Frequencies and Mode Shapes using Vibration Isolator to Transport "Satellite Model–Plate Connecting Interface" System

Abbas Waheed Dahham[1], Pavel Alexandrovich Taranenko[2] and Aleksey Victorovich Erpalov[2]

[1] Faculty of Mechanical Engineering, Pavlodar State University, Kazakhstan
[2] Faculty of Aerospace, South Ural State University, Russia

E-mail: taranenkopa@susu.ru

Abstract. This paper examines the natural frequencies and mode shape numerically and experimentally using vibration isolator for satellite model-plate connecting interface. The experiment was carried out using a modern software and hardware complex LMS. Vibration accelerations on the object were measured at 13 points in three mutually perpendicular directions using one-component and three-component PCB accelerometers with a sensitivity of 100 mV/g. Excitation was carried out with a PCB 086D50 m modal hammer. The SCADAS mobile data acquisition system was utilized to record the response from the sensors. While the numerical calculations were performed in the finite element package ANSYS Workbench. The result shows that the natural frequencies are less dependent on the system damping where the most considerable difference (about 10%) is observed in those forms, which plate makes flexural vibrations; the six natural modes of vibration of the satellite model (as a rigid body), the first three lowest forms correspond to vibrations in the plane. While the other oscillations were out of the plane, to reduce the oscillation frequency of the product from the plane (around the x and z axes), it is recommended to reduce the distance between the shock absorbers.
Keywords. Transport satellite, Vibration isolator.

1. Introduction

Undesired vibrations in engineering practices consider very harmfully to any type of structure and machinery [1]. To reduce undesired oscillations, many different forms of vibration isolation systems are used. The initial data to calculate the natural frequencies and vibration mode shapes of any vibration isolator system are the vibration isolator stiffness characteristics that use to decline undesired oscillations of the sensitive mobile equipment. For example, many studies tried to reduce the vibrations in complex systems such as heavy rotary and piston machines, aviation electronics, ship equipment, and various vibration-sensitive devices where the vibration isolator was used. The cable shock absorber contains an elastic element in the form of a spiral made of a steel cable and two metal plates with holes for the cable, installed on two metal plates. The dry friction for the cable uses to reduce vibration amplitude. Also, the locations of the vibration isolators in the system are considered to ensure that the vibration frequencies fall within the range of 8 - 10 Hz in the x-z plane of the product (horizontal plane) for all three frequencies of oscillations in the plane; this condition is vital to

Content from this work may be used under the terms of the Creative Commons Attribution 3.0 licence. Any further distribution of this work must maintain attribution to the author(s) and the title of the work, journal citation and DOI.
Published under licence by IOP Publishing Ltd

keep the electronic instruments save without damages during transportation. In addition to the presentation of vibration protection systems, many articles are devoted to finding modern methods to calculate the natural frequencies and mode shapes using finite element packages [2, 3, and 4]. The article [2] provides a nonlinear analysis of the natural frequencies of the simplest vibration isolator. The analysis is carried out without the use of empirical research. The calculation results and the design diagram of the vibrio-isolator are shown in Figure (1).

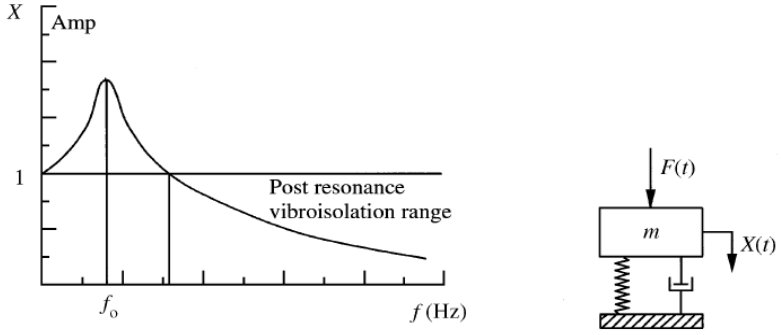


Figure 1. The frequency response of a simple vibration isolator.

The figure shows that the zones of amplification and attenuation of oscillations and the resonant frequency f_0. Also, calculations of a more complex vibration isolation system were carried out without load and with load, as shown in Figures 2 and 3.

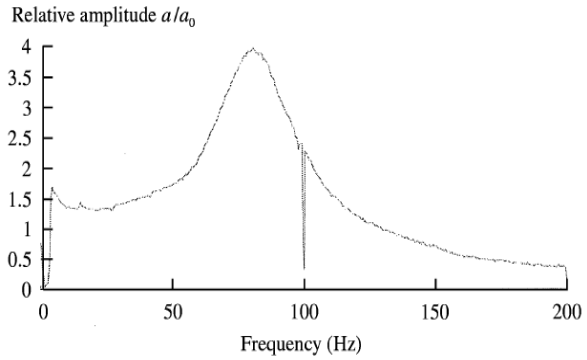


Figure 2. No-load vibration isolation function.

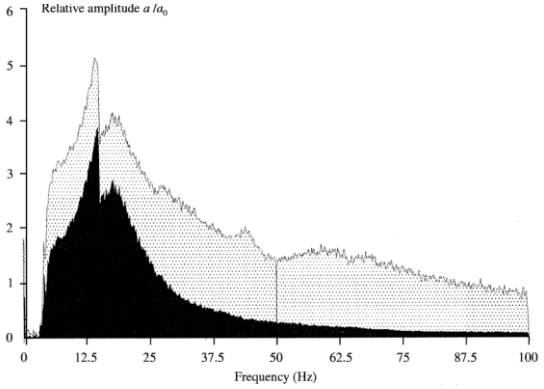


Figure 3. Vibration isolation function under static load 80 N (black) and 100 N (white).

Vibration damping device CAVOFLEX (Cavoflex Shock and Vibration Mounts with outstanding features, Schiff and Hafen No. 10. 1988) [1] by Willbrandt Gummitechnic is made of a spiral of a steel cable (from now on it is referred to as a cable) and two pairs of plates, fastened to each other by a threaded connection in a diametric - opposite points of the spiral circle, Figure 4.

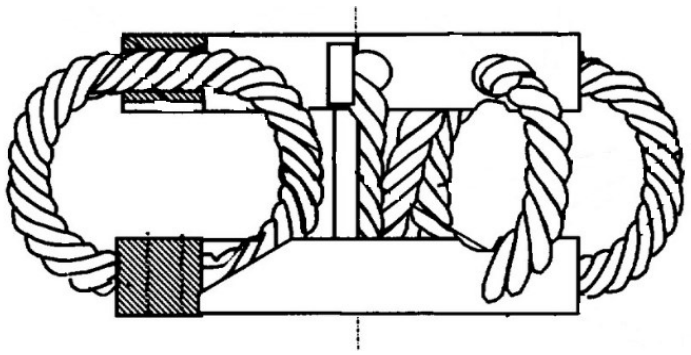


Figure 4. Vibration damping device CAVOFLEX.

Invention by A.S. USSR No. 1588938 contains an elastic damping element in the form of a cable spiral and two pairs of metal plates. The plates are installed on the turns of the rope spiral from the outer and inner sides at diametrically opposite points of the spiral circle. In each pair of plates, the outer and inner plates are fastened with fasteners (screws), and due to the selected shape of the inner plates, additional elastic elements are located between them, which makes it possible to increase the shear stiffness of the vibration damping device without increasing its dimensions. In this paper, the evaluation of the natural frequencies of the satellite model will be investigated numerically and experimentally considering the suspension stiffness and estimate the lowest frequencies of natural vibrations (as of a solid) of the system "satellite-model - connecting interface plate" on the vibration isolation system [5-8], also comparison and comparative analysis of calculation and experimental results.

2. Governing equation

We will perform an analytical selection of the parameters of the vibration isolation system. The number of fixing points for elastic supports is 4. We assume that the platform is rigid; its flexibility will be considered in the subsequent calculation with a finite element. The design diagram of the product on the vibration isolation system with vertical translational vibrations in the direction of the y-axis is shown in Figure 5, and its equivalent model is shown in Figure (6). With translational vertical vibrations, the platform plane remains parallel to the z-x plane, and the natural vibration frequency of the system shown in Figure (6) depends on the suspension stiffness and the platform mass and is determined by the following expression

$$f_y = \frac{1}{2\pi} \cdot \sqrt{\frac{c_{y\Sigma}}{m_{pl}+m_{pro}}} \text{Hz} \quad (1)$$

With translational vertical vibrations must perform condition in Equation (2) below:

$$[f_1]_{min} \leq f_y \leq [f_1]_{max}$$

$$10 \text{ Hz} \leq f_y \leq 13\ Hz \quad (2)$$

From Equation (1) the stiffness of the suspension in terms of the platform mass and natural frequency

$$c_{y\Sigma} = \left(m_{pl} + m_{pro}\right) \cdot \left(2\pi \cdot f_y\right)^2, \text{N/m} \quad (3)$$

Now, setting the permissible minimum $[f1]_{\text{min}}$ and maximum $[f1]_{\text{max}}$ natural frequencies, we find that the corresponding boundaries of the suspension stiffness range in the direction of the y-axis from the condition that the natural frequency of vertical translational vibrations falls into the permissible range of 10-13 Hz

$$c_{y\Sigma_{min}} = \left(m_{pl} + m_{pro}\right) \cdot (2\pi \cdot [f_1]_{min})^2, \text{N/m} \quad (4)$$

$$c_{y\Sigma_{max}} = \left(m_{pl} + m_{pro}\right) \cdot (2\pi \cdot [f_1]_{max})^2, \text{N/m} \quad (5)$$

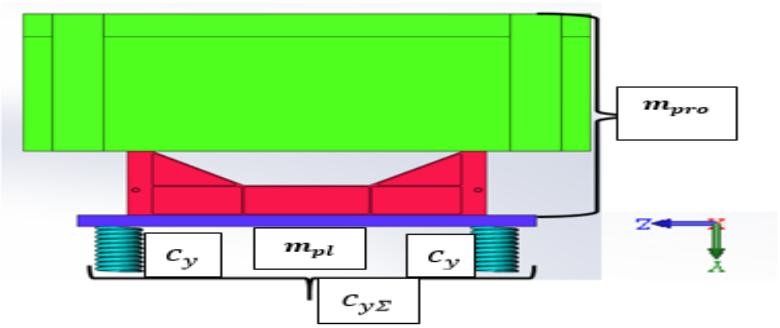


Figure 5. Design diagram of a product on a vibration isolation system with vertical translational vibrations in the direction of the *y*-axis.

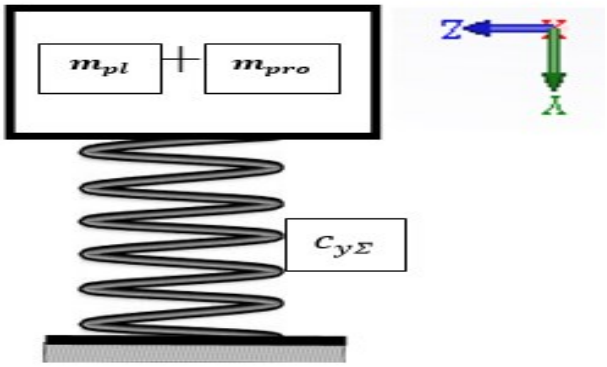


Figure 6. Equivalent model of a product on the vibration isolation system with vertical translational vibrations (in the y-axis direction).

We obtain similar dependencies for translational vibrations in the longitudinal and transverse directions and find the corresponding boundaries of the suspension stiffness range in the direction of the x and z axes from the condition that the natural frequencies of the longitudinal and transverse translational vibrations fall into the permissible range of 8–10 Hz:

$$c_{x\Sigma_{min}} = c_{z\Sigma_{min}} = (m_{pl} + m_{pro}) \cdot (2\pi \cdot [f_2]_{min})^2, \text{ N/m} \quad (6)$$

$$c_{x\Sigma_{max}} = c_{z\Sigma_{max}} = (m_{pl} + m_{pro}) \cdot (2\pi \cdot [f_2]_{max})^2, \text{ N/m} \quad (7)$$

Expressions in Equations (4), (5), (6), depending on the mass of the plate, are given in Figure (7), dependence (7) coincides with (5) and is not shown in Figure (7)).

Figure (7) should be used as follows, with the known mass of the plates is carried out with total stiffness selection of suspension: The total stiffness of the suspension in the vertical direction should be located between two curves corresponding to 10 and 13 Hz. The total stiffness of the suspension in the longitudinal (transverse) direction should be located between two curves corresponding to 8 and 10 Hz.



Figure 7. The total stiffness of the suspension.

3. Experimental procedure

The experimental determination of the vibration frequencies and mode shapes of the satellite model was carried out using the modern software and hardware complex LMS. Vibration accelerations on the object were measured at 13 points in three mutually perpendicular directions using one-component and three-component PCB accelerometers with a sensitivity of 100 mV/g. Excitation was carried out with a PCB 086D50 modal hammer. The response from the sensors was recorded by the SCADAS Mobile data acquisition system. LMS Test. Lab v13 package, Impact Testing module, was used as software. Four measurement points 1-4 are selected at the edges of the connecting interface plate and one in the middle of plate 5, one more - at the top of the satellite model 5 and three points each on the upper rods (ends and middle) 7-10, 61, 62. Additional point 55 to excite the vibration modes of the load-model in the plane - the center of mass of the object. The installation points of the accelerometers ("wire" model) are shown in Figure (8).

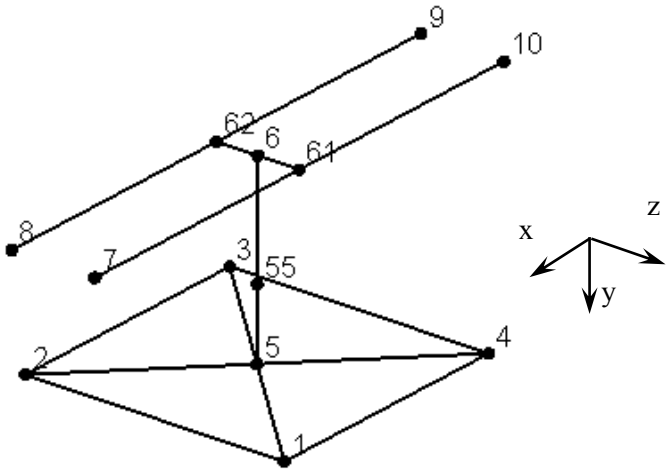


Figure 8. Installation points of accelerometers ("wire" model).

To experimentally determine the modes of vibration of the satellite model as a solid, the excitation of vibrations was carried out by hitting using the modal hammer in succession at three points: along the x and z axes at point 55 and along the y-axis at point 6. The vibrations' natural forms and frequencies of the satellite model were determined for different positions of the vibration isolators. Selected four positions of vibration isolators, Figure 9.

Location 1- The x-axis of each vibration isolator is directed from the attachment point to the center of the connecting interface plate;

Location 2- The x-axis of each vibration isolator is rotated around the vertical axis by 90 degrees relative to location 1;

Location 3- The x-axes of vibration isolators are oriented along the direction of movement (along the axes of the rods of the satellite -model);

Location 4- The x-axes of vibration isolators are oriented perpendicular to the direction of movement (perpendicular to the axes of the rods of the satellite model).

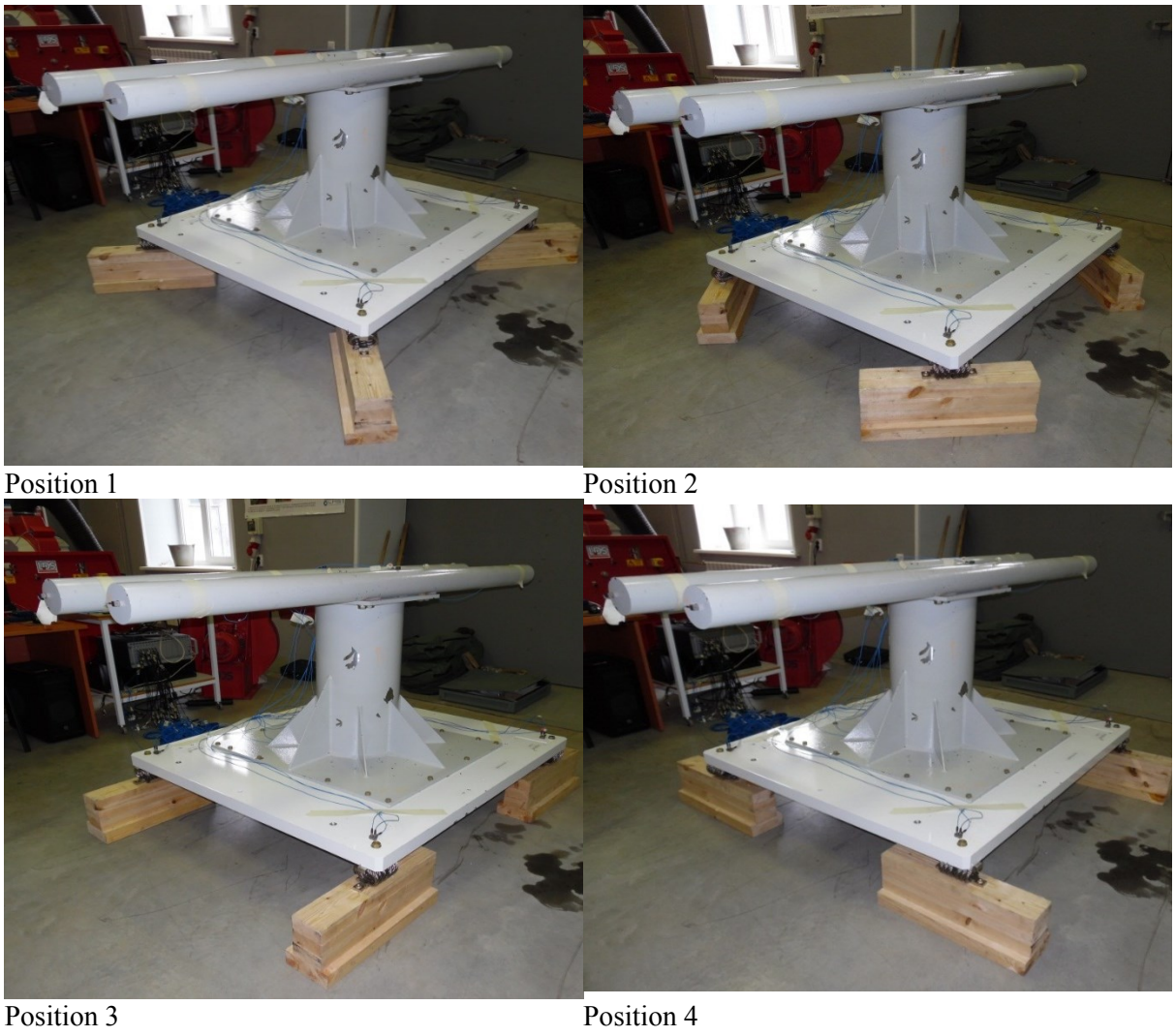


Figure 9. Positions of vibration isolators.

Accurate identification of vibration frequencies corresponding to certain forms is difficult experimentally; therefore, the work revealed an estimated frequency range, wherein unequivocally, there is a form of vibration of the satellite-model.

4. FEA Methodology

A three-dimensional model was built in the SolidWorks engineering package based on the approved drawings of the satellite-model with the connecting interface plate. The numerical calculation of the natural frequencies and mode shapes of the research's object was performed in the finite element package based on ANSYS Workbench. The imported object solid geometric model was broken into finite elements with a size of 20 mm. In places where vibration isolators were installed, concentrated elastic elements were located in three directions x, y, and z. The z-axis of the shock absorbers is directed along the y-axis of the product. The stiffness of the shock absorber in the transverse directions is taken equal to 0.25 and 0.3 of the stiffness in the vertical direction Table (1). The stiffness characteristics of the springs were set in accordance with Table 1. The design model of the satellite model is shown in Figure (10) and Figure 11.

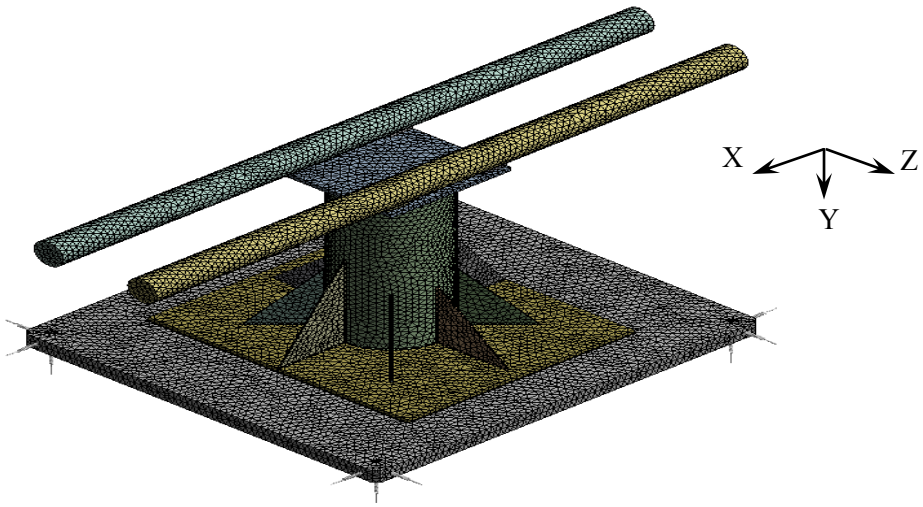


Figure 10. The build finite element model of the research object.

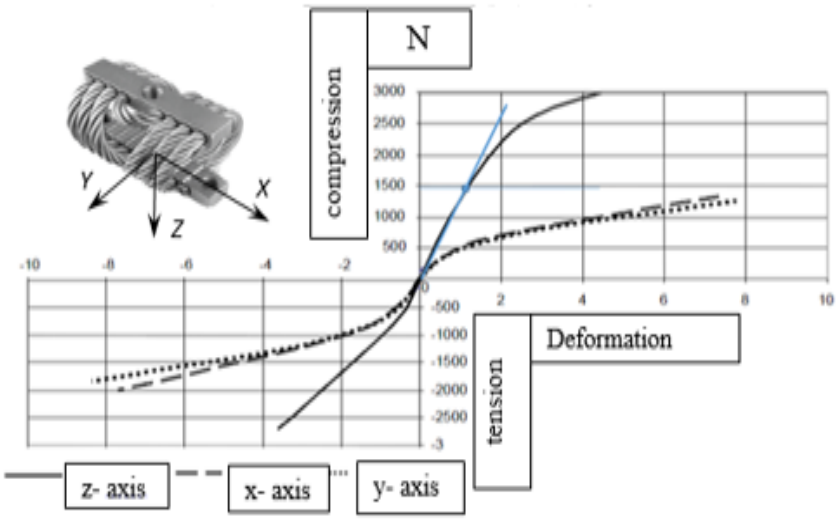


Figure 11. Estimated stiffness of the vibration isolator.

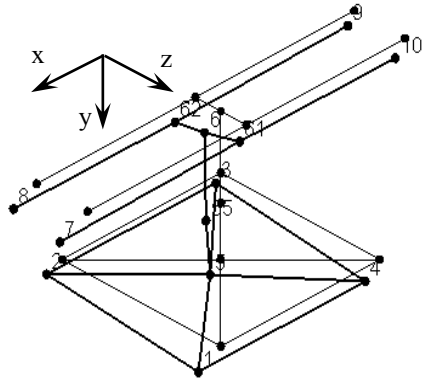
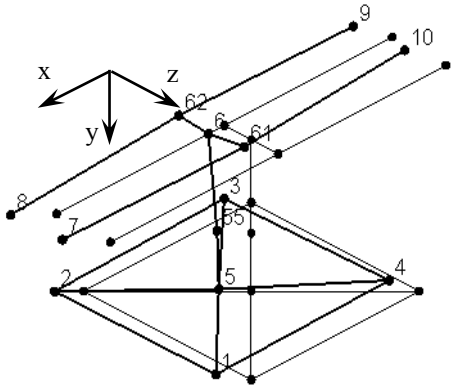
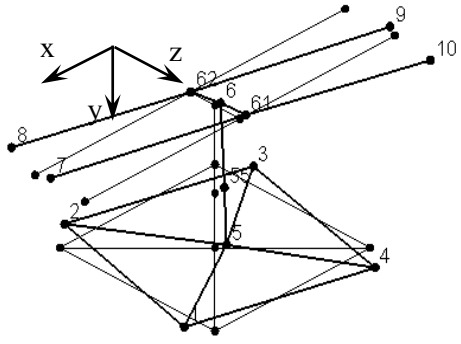
Table 1. Isolator stiffness.

Axial stiffness	Value, N / mm
The stiffness of the shock absorber axis Z	1300
The stiffness of the shock absorber axis X	390
The stiffness of the shock absorber axis Y	325

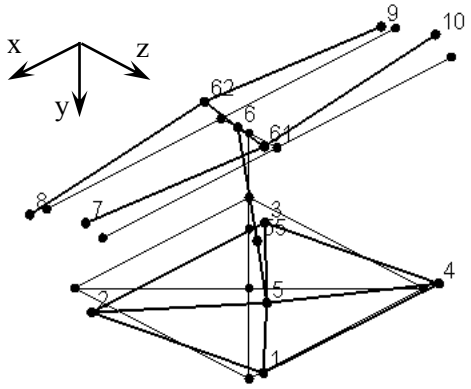
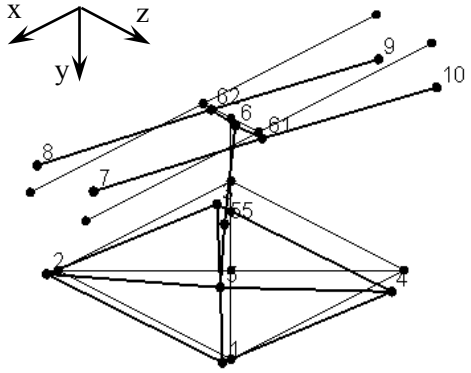
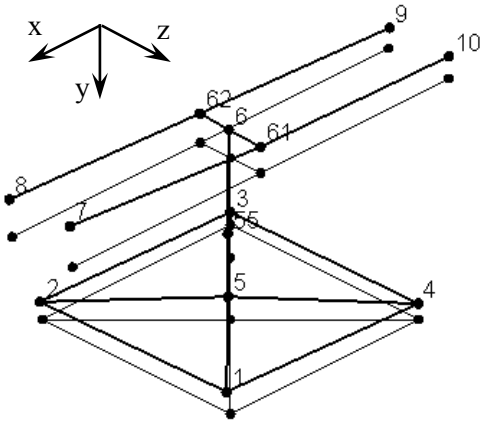
5. Results and discussion

The natural frequencies of the object as a rigid body obtained experimentally for the four isolators are presented in Table (2). It is experimentally challenging to identify the vibration frequencies corresponding to certain forms accurately; therefore, an estimated frequency range has been identified in work, in which the form of vibration of the satellite model is unambiguously present.

Table 2. Experimental ranges of frequencies and mode shapes of natural vibrations of a prototype product as a rigid body with vibration isolators.

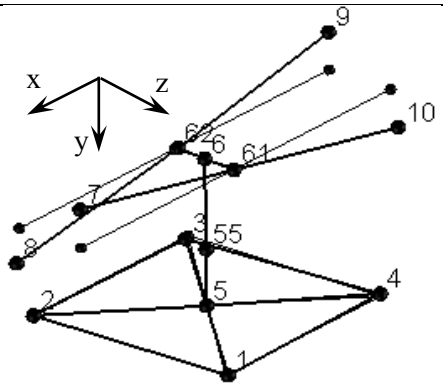
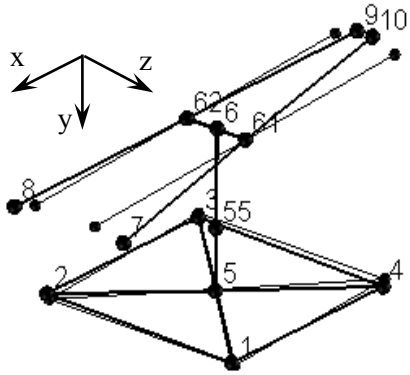
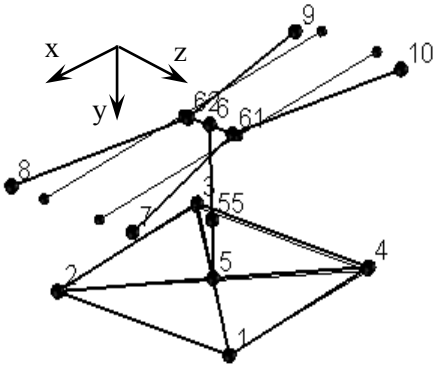
Natural frequency range, Hz				Vibration natural mode shape
1 position	2 position	3 position	4 position	
8,8-9,8	7,5-8,7	10,3-11,2	5,1-5,6	 Vibrations along the x-axis
8,3-10,5	8,4-10,0	5,6-5,9	10,3-11,8	 Vibrations along the z-axis
10,5-11,2	17,1-20,2	14,9-16,2	13,0-15,4	 Vibrations along the y-axis

Continue …

26,1-28,9	26,2-27,1	25,2-26,3	27,1-29,5	
				Vibrations around the x-axis
21,31-22,0	19,6-21,7	21,9-23,1	17,4-21,1	
				Vibrations around the z-axis
20,5-20,8	19,2	19,8-20,4	20,3-21	
				Vibrations around the y-axis *y*

The natural vibration frequencies of the test object above 40 Hz, obtained experimentally, for four vibration isolator locations are presented in Table (3) and (4).

Table 3. Experimental frequencies and mode shapes of natural vibrations of a prototype product with vibration isolators.

Natural frequency range, Hz				Vibration natural mode
1 position	1 position	1 position	1 position	
44,413	44,400	44,454	44,407	 Vibrations of rods in antiphase in the direction of the y-axis
63,418	62,408	63,522	62,751	 In-phase vibration of the rods in the direction of the y-axis
68,993	68,499	68,524	68,442	 Vibrations of rods in antiphase in the direction of the z-axis

Continue …

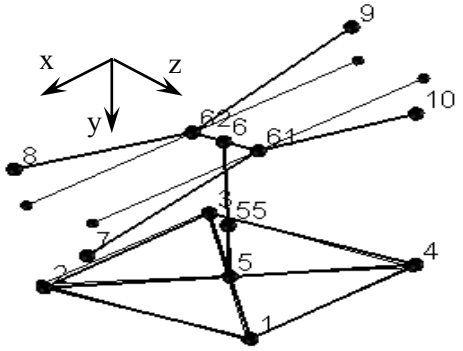
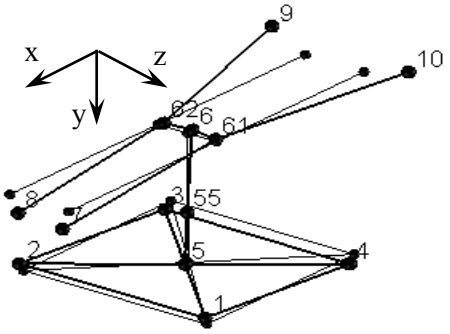
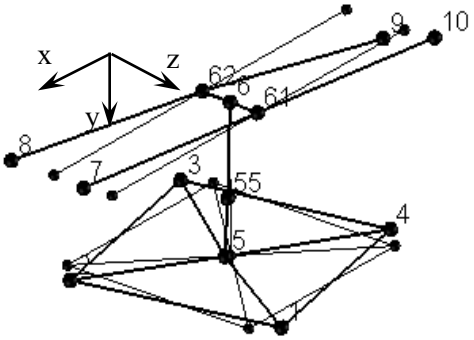
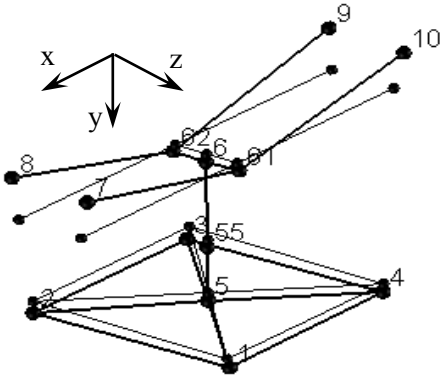
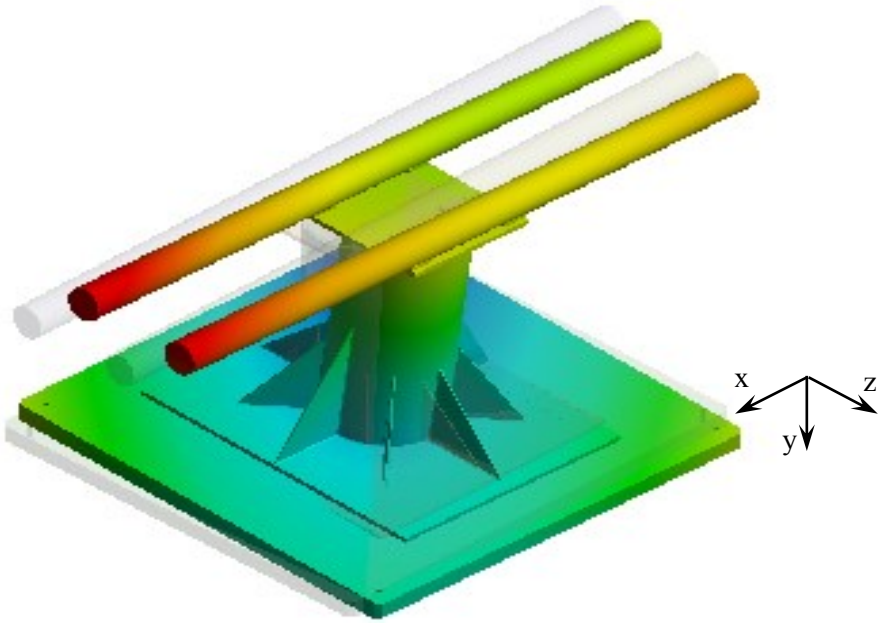
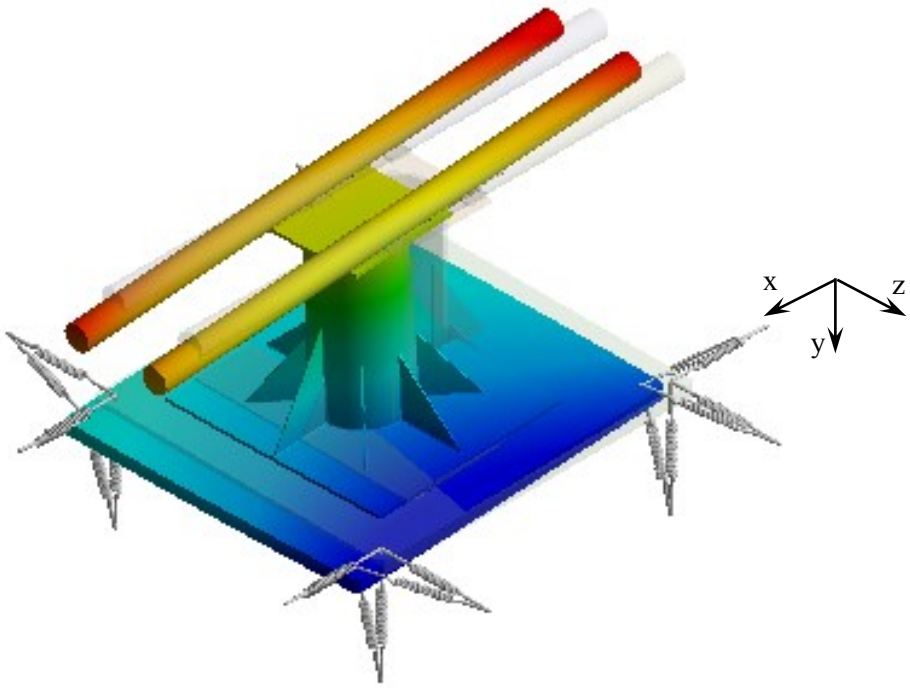
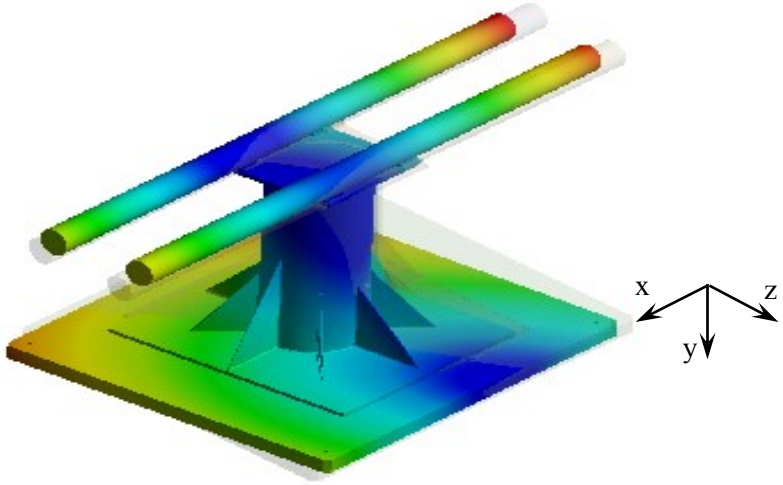
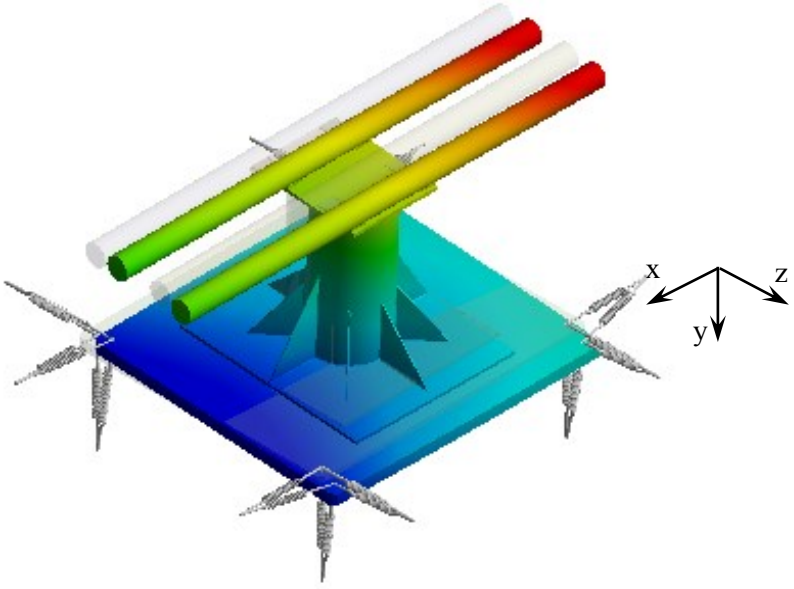
74,668	74,601	74,612	74,510	 Vibrations of the rods in antiphase in the direction of the y-axis with the swing of the plate around the x-axis
71,651	70,540	71,679	70,995	 Vibrations of rods in antiphase in the direction of the *z*-axis with oscillating plate and rods around the z-axis
82,457	84,621	83,752	82,089	 Torsional vibrations of the product around the y-axis
85,450	85,298	85,600	85,463	 Vibrations of the product in the direction of the y-axis

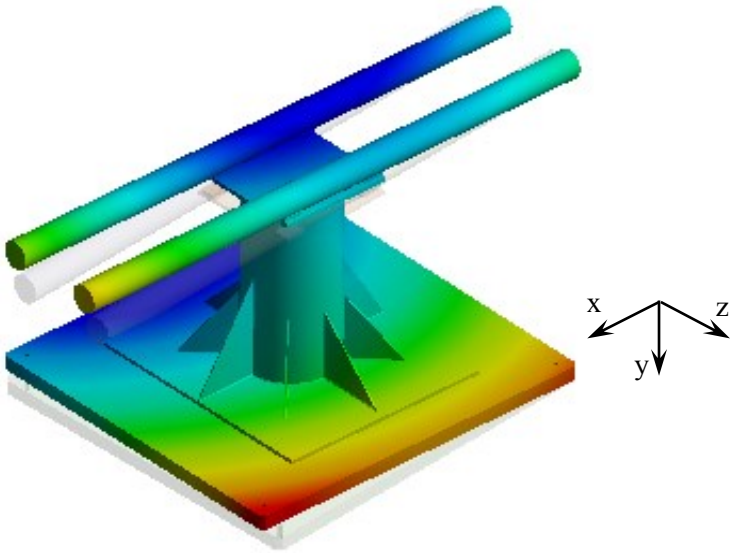
Table 4. Calculated natural vibration frequencies with installed vibration isolators without vibration isolators when the satellite model weight is 550 kg.

	Natural vibration frequency, Hz	Vibration natural mode
Calculation without vibration isolators	0	
Calculation with vibration isolators	10,551	
		Vibrations of the product along the z-axis

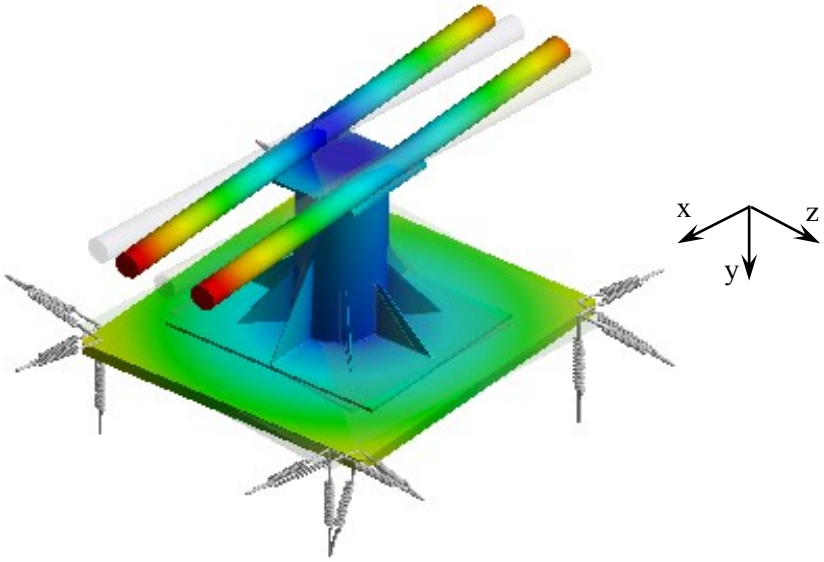
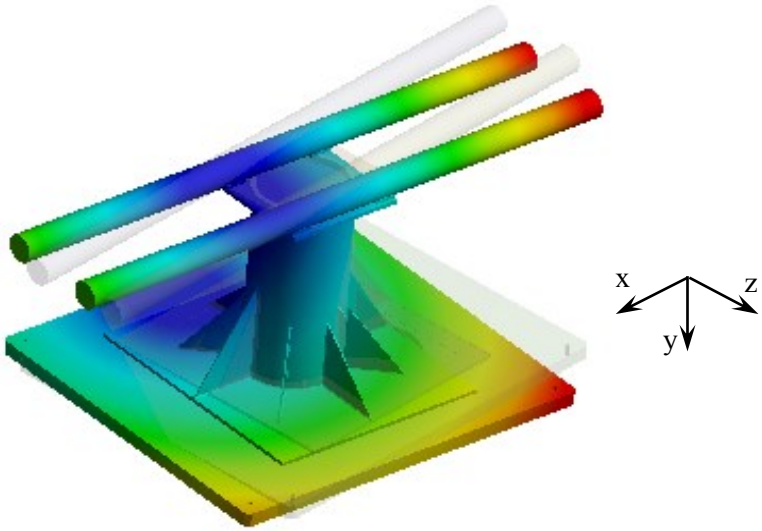
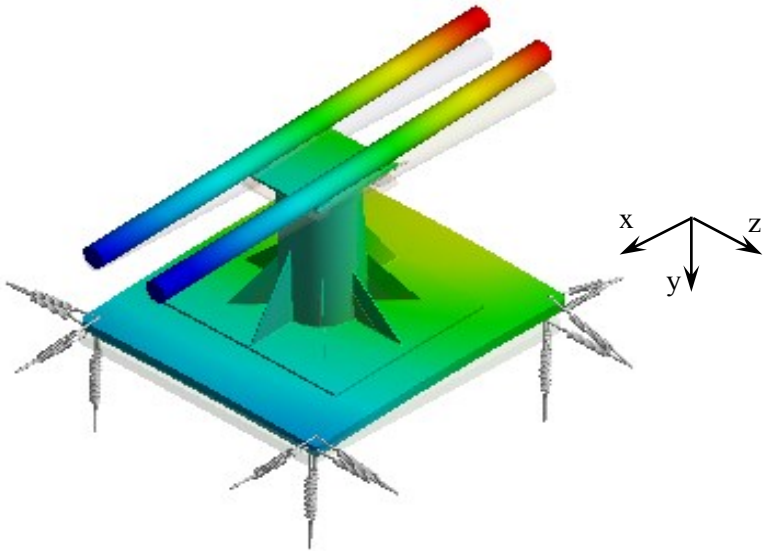
Continue …

Calculation without vibration isolators	0	
Calculation with vibration isolators	11,226	

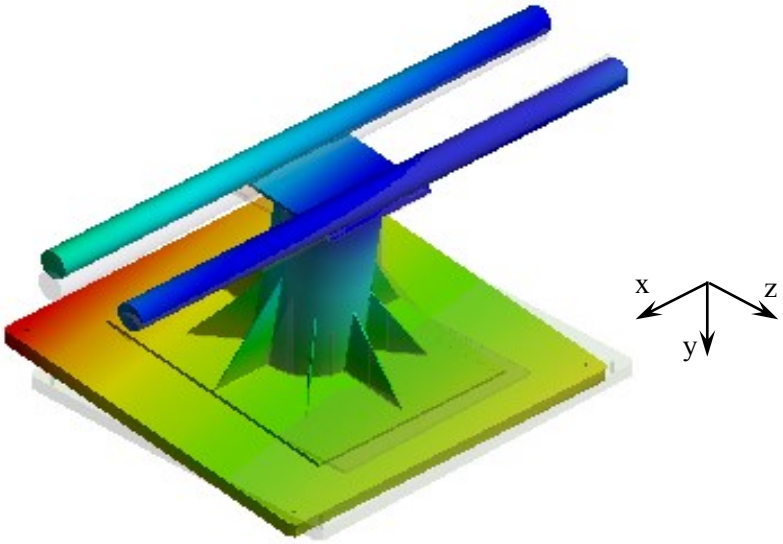
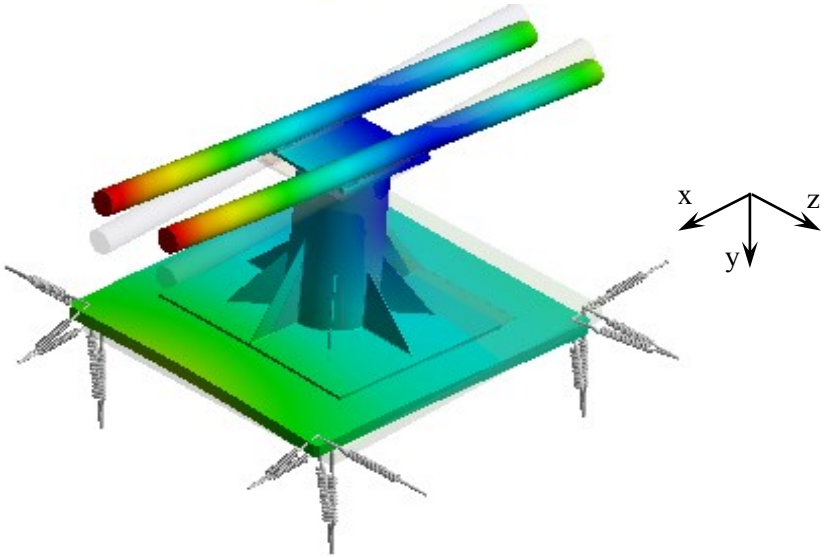
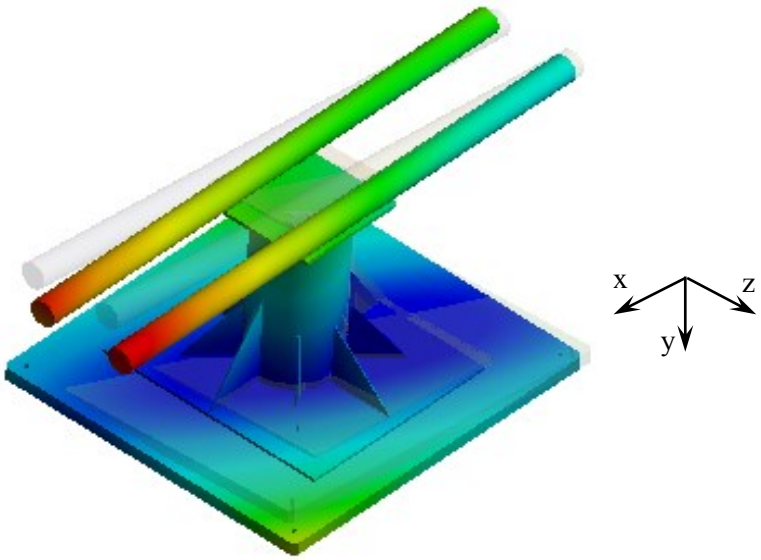
Vibrations of the product along the x-axis

Calculation without vibration isolators	0	

Continue …

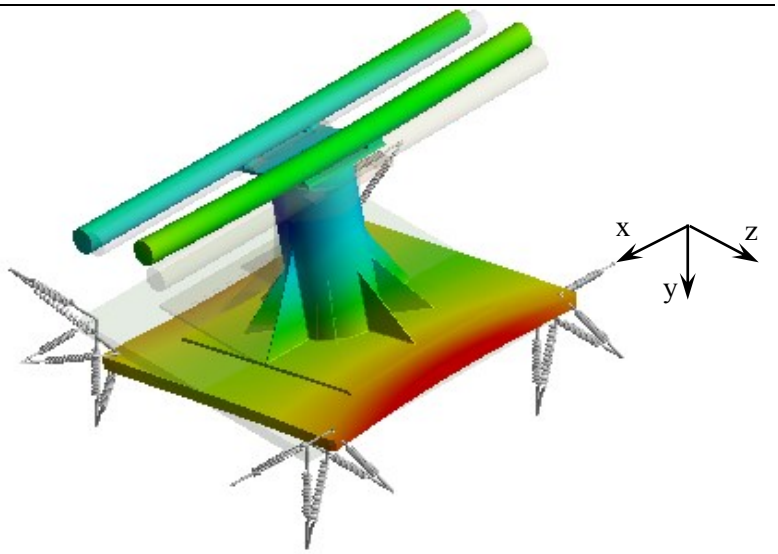
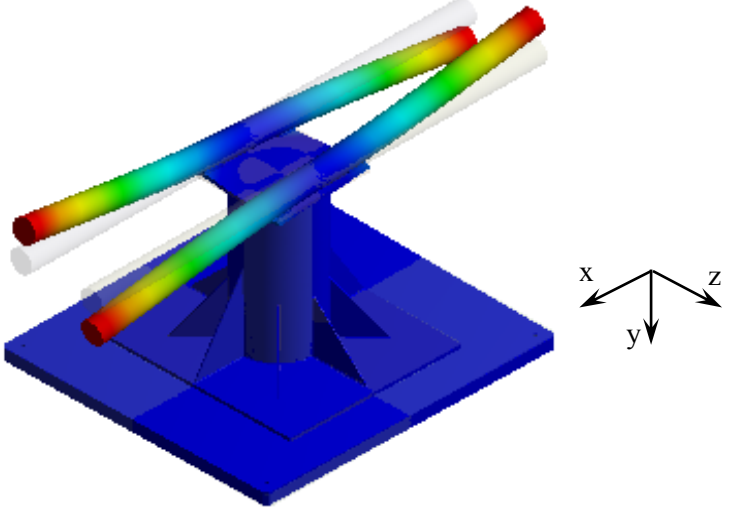
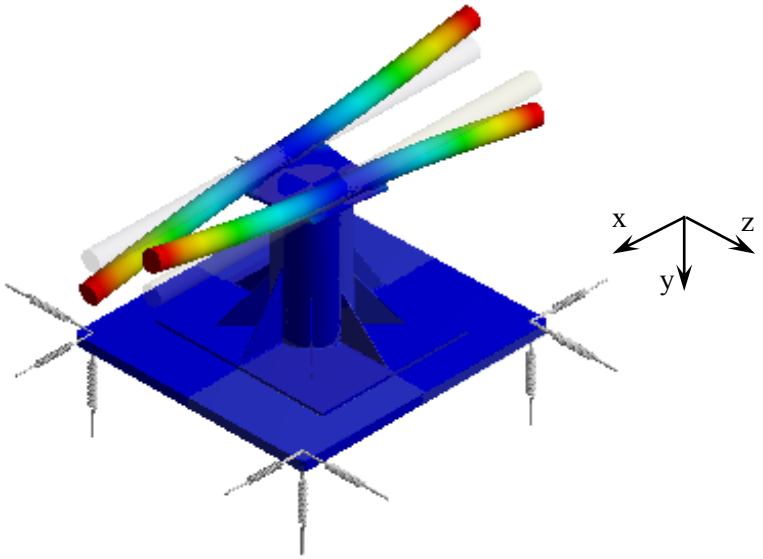
Calculation with vibration isolators	18,712	 Vibrations of the product around the axis *y*
Calculation without vibration isolators	5,3424e-004	
Calculation with vibration isolators	20,004	 Vibrations of the product along the y-axis

Continue …

Calculation without vibration isolators	9,2946t-004	
Calculation with vibration isolators	22,359	
Calculation without vibration isolators	1,4205e-003	

Vibrations of the product around the z-axis

Continue …

Calculation with vibration isolators	28,412	 Vibrations of the product around the x-axis
Calculation without vibration isolators	54,641	 Vibrations of rods in antiphase in the direction of the y-axis
Calculation with vibration isolators	54,699	 Vibrations of rods in antiphase in the direction of the y-axis

When we changed the positions of the shock absorbers experimentally, we found that the frequency changed in the Z fraction was 14.9-16.2 Hz, became 13 Hz, Figure 12 and Table 5.

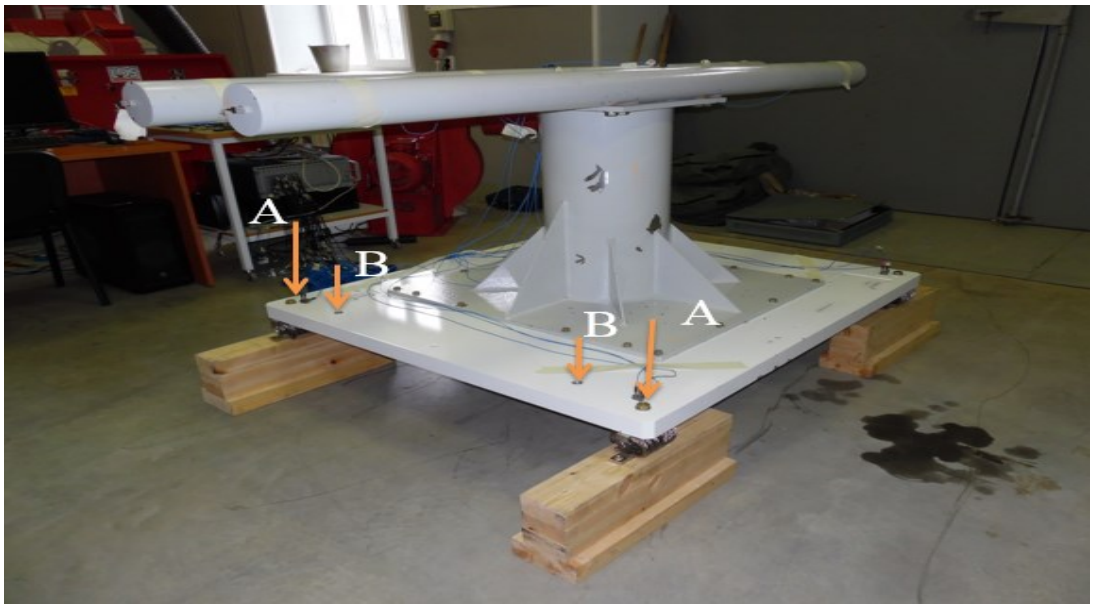
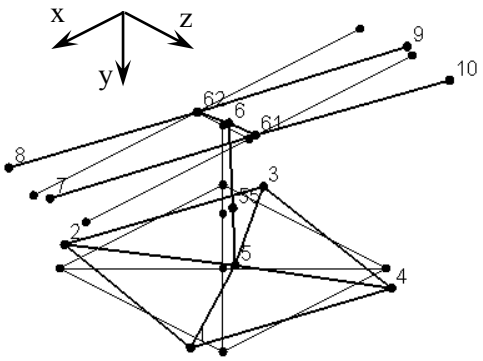


Figure 12. Location of shock absorbers (A - it was; B - it became).

Table 5. Experimental ranges of frequencies and forms of natural vibrations of a prototype product with vibration isolators as a solid.

1 Position	2 Position	3 Position	4 Position	
10,5-11,2	17,1-20,2	13	13,0-15,4	
				Vibrations around the y-axis

6. Conclusion

1. A preliminary calculated estimate of the natural frequencies of the product on the vibration isolators shows that for the six natural mode shapes of vibration when the satellite model as an absolutely rigid body, the first three lowest forms correspond to vibrations in the plane, the fourth, fifth and sixth - vibrations from the plane. This fact is confirmed experimentally.
2. A preliminary calculated estimate of the product's natural frequencies on the vibration isolators shows that the product's natural frequencies, at which the product begins to deform, are less dependant on the damping system. The most significant difference (about 10%) is observed for those forms where the plate shows bending vibrations.

3. As the experiments showed, when using shock absorbers, depending on the orientation of the shock absorbers, we could obtain the natural vibration frequencies of the product as an absolutely rigid body from 5 to 20 Hz in the *x-z* plane. Positions 3 and 4 provide the lowest vibration frequency of the product as a completely rigid body of about 5 Hz (vibrations along or across the direction of movement).

To ensure that the lowest natural frequency falls into the range of 8-10 Hz in the *x-z* plane, it is necessary to use arrangement 1 or 2. So, at locations 1 or 2, the natural frequencies of the product along and across the direction of movement differ insignificantly, and as average, they fall into the range of 8-10 Hz. In this case, the natural frequency of the product in the plane, which corresponds to the vibration shape around the vertical axis, is about 10-11 Hz at location 1 and 17-20 Hz at location 2. In order to get into the range of 8 - 10 Hz when oscillating in the *x-z* plane of the product (horizontal plane) for all three in-plane frequencies, it is recommended to use location 1.

4. It has been experimentally established that the orientation of the shock absorbers in the plane (locations 1 - 4) practically does not affect the product's natural mode shapes.
5. It has been experimentally established that the two lowest frequencies from the plane correspond to the vertical translational oscillations and rotate around the perpendicular axis to the movement direction. These two frequencies are close to each other and are about 19-21 Hz. The third frequency, corresponding to oscillations around the movement direction, is about 26-29 Hz.

The stiffness of the damping system determines the frequencies of vertical vibrations in the z-axis of the shock absorber. It can be reduced by using more flexible shock absorbers, but a decrease in the shock absorbers stiffness will lead to the fact that vibration frequencies in the plane will go out of the permissible range (8-10 Hz). The angular vibration frequencies are determined by the moments of inertia of the product around the *x* and *z* axes and the distances between the shock absorbers. The oscillation frequencies of the product around the *x* and *z* axes are directly proportional to the shock absorbers' distance. Therefore, to reduce the oscillation frequency of the product from the plane (around the *x* and *z* axes), it is recommended to reduce the distance between the shock absorbers.

To solve the problem of falling into the 10-13 Hz range of the lowest of the three natural vibration frequencies from the plane, it is necessary to reduce the distance between the shock absorbers along the direction of motion.

To solve the problem of reducing the maximum natural frequency (about 26-29 Hz), it is necessary to reduce the distance between the shock absorbers across the direction of movement.

Nomenclature

y	Vertical Axis.	
x	Longitudinal Axis (in the Direction of Transport Movement).	
z	Transverse Axis (Complements the Coordinate System to the Right).	
$[f_1]_{min}$	The Minimum Permissible Natural Frequency of the Product Oscillations on Shock Absorbers During Its *ZX* Plane Oscillations.	Hz
$[f_1]_{max}$	The Maximum Permissible Natural Frequency of the Product Oscillations on the Shock Absorbers During Its *ZX* Plane Oscillations.	Hz
$[f_2]_{min}$	Minimum Permissible Natural Frequency of the Product Oscillations During Its *ZX* Plane Oscillations.	Hz
$[f_2]_{max}$	The Maximum Permissible Natural Frequency of the Product Oscillations During Its *ZX* Plane Oscillations.	Hz
f_y	Natural Frequency of the Product Oscillations on Shock Absorbers During Product During Its *Y*-Axis Oscillations.	Hz
g	Acceleration Due to Gravity.	m / s^2
m_{pro}	Product Weight Together with the Connecting Interface Plate.	kg
m_{pl}	Platform Weight.	kg
c_y	Stiffness of One Shock Absorber in the *Y*-Axis Direction.	N / m
$c_{y\Sigma}$	Total Stiffness of the Suspension in the *Y*-Axis Direction.	N / m
$c_{y\Sigma min}$	Minimum Permissible Total Stiffness of the Suspension in the *Y*-Axis Direction.	N / m
$c_{y\Sigma max}$	Maximum Permissible Total Stiffness of the Suspension in the *Y*-Axis Direction.	N / m

7. References

[1] S M Mahdi Mofidian and Hamzeh Bardaweel 2017 *Displacement Transmissibility Evaluation of Vibration Isolation System Employing Nonlinear-Damping and Nonlinear-Stiffness Elements* (Journal of Vibration and Control) vol 24 pp 4247–4259

[2] Bezrukikh S S, Golovenkin E N, Melkomukov A A and A V Zeitler 2009 *Antipiev A.I. Problems of Reducing the Negative Impact of Mechanical Loads on the Spacecraft During Its Transportation* (Conference "Reshetnev Readings", Krasnoyarsk) p 293

[3] Makarenkov A I and Slepov A V 2007 *Rope Shock Absorber And Method of its Manufacture (Options)* (Patent RF, No 2305809,Moscow)

[4] Danabalan T N et al 2011 *Safety Systems for Satellite Transportation*

[5] Zielnica J, Ziółkowski A, Cempel C 2003 *Nonlinear Vibroisolation Pads FEM Analysis and Introductory Experimental Investigations* (Mechanical systems and signal processing)vol T 17 no 2 pp 409–422

[6] Brincker R, Zhang L, Andersen P 2001 *Modal Identification of Output-Only Systems Using Frequency Domain Decomposition* (Smart materials and design, numerical structures) vol T 10 no 3 p 441

[7] IVANCU B et al 2015 *Harmonic Analysis of a Vibrating Feeder Using "Linear Dynamics" Module* (Proceedings of the 43rd International Symposium on Agricultural Engineering, Actual Tasks on Agricultural Engineering, Opatija, Croatia, 24-27 February 2015, University of Zagreb) pp 505–511

[8] Testoedov N A et al 2013 *Some Aspects of Design, Manufacturing Technology, Testing and Operation of Depreciation Platforms for Fixing Automatic Spacecraft in a Transport Container* (Bulletin of SibGAU) vol 6 no 52 pp 173–179